Horizontal Diffusion Characteristics in Lake Ontario

C. R. MURTHY

Applied Research Division, Canada Centre for Inland Waters, Burlington, Ontario

(Manuscript received 19 February 1975, in revised form 8 August 1975)

ABSTRACT

Experimental data on the diffusion of fluorescent dye patches were obtained in Lake Ontario, to study large-scale horizontal diffusion characteristics. In each experiment, a slug of water-soluble rhodamine dye solution was introduced at appropriate depths. The growth of the diffusing dye patch was followed up to 80 h after dye release, using fluorometric sampling. The data covered a length scale (i.e., patch size) of 100 m to 15 km and the corresponding eddy diffusivities varied from 10^2 to 10^6 cm^2 s^{-1}. Several horizontal diffusion characteristics are constructed based on a simple theoretical framework. Although the diffusion characteristics cannot be justified entirely from theoretical arguments, they could be viewed as purely statistical since they have been constructed from experimental data obtained in widely varying environmental conditions and provide useful guidelines for modeling practical diffusion problems.

1. Introduction

The circulation in natural bodies of water such as the oceans and the Great Lakes are generally very complex turbulent motions. Superimposed on the mean flow circulation patterns are eddy-like motions of varying intensity and scales. These eddy-like motions exist in both horizontal and vertical directions. The scale of horizontal eddies, however, are much larger than the vertical eddies because the Lakes (or the oceans) are many times wider than they are deep. A direct consequence of this is the large-scale water movements and the associated transport and dispersion of chemical and biological species from one area of the lake to another. The practice of discharging municipal and industrial wastes including waste heat from thermonuclear power plants (and radioactive materials into the oceans) provided impetus for extensive theoretical and experimental studies of turbulent diffusion processes in natural bodies of water. However, turbulent diffusion processes are complex and theoretical predictions of dispersion of these wastes are far from satisfactory. Thus, an understanding of the various manifestations of turbulent diffusion processes is largely dependent on the empirical approach of conducting field diffusion experiments. With this objective in mind several large-scale diffusion experiments were carried out during MELON[1] (1969) and IFYGL[2] (1972) in Lake Ontario.

2. Experiments

The experimental technique consisted of generating a "dye patch" at selected depth by instantaneous release of a slug of rhodamine B dye solution and following the subsequent diffusion of the dye patch as the lake currents and their eddies caused it to spread and dilute. The density of rhodamine B dye solution (40% acetic acid) was adjusted to the *in situ* density by adding methanol and surface water. Water samples taken at selected depths of dye solution were used to determine the *in situ* density. No attempt was made to adjust the temperature of the dye solution to the *in situ* temperature, and usually the initial mixing during the injection was sufficient to compensate for the temperature difference. The details of the method of dye release and the fluorometric sampling of the dye patch have been described earlier (Murthy, 1970, 1973; Kullenberg, 1971, 1972). A total of 12 experiments were carried out in the epilimnion[3], thermocline and hypolimnion[4] under a wide variety of environmental conditions. Fig. 1 shows the geographic distribution of the experiments. Some general details of the experiments are summarized in Tables 1 and 2. The experiments covered time scales up to 80 h and spatial (horizontal) scales up to 15 km.

3. Data analysis

As remarked in the Introduction, the horizontal scales of motions in the Lakes and oceans are much greater than the vertical scales and therefore, in many cases, their effect on mixing may be considered separately. This idea has been explored by a number of investigators with considerable success. In this approach it is assumed that the introduced substance is subject to horizontal mixing within a sufficiently thin homogeneous layer so

[1] Massive Effort on Lake Ontario: an IFYGL feasibility study.
[2] International Field Year for the Great Lakes.
[3] Upper mixed layer of the lake.
[4] Deep layer, below the thermocline.

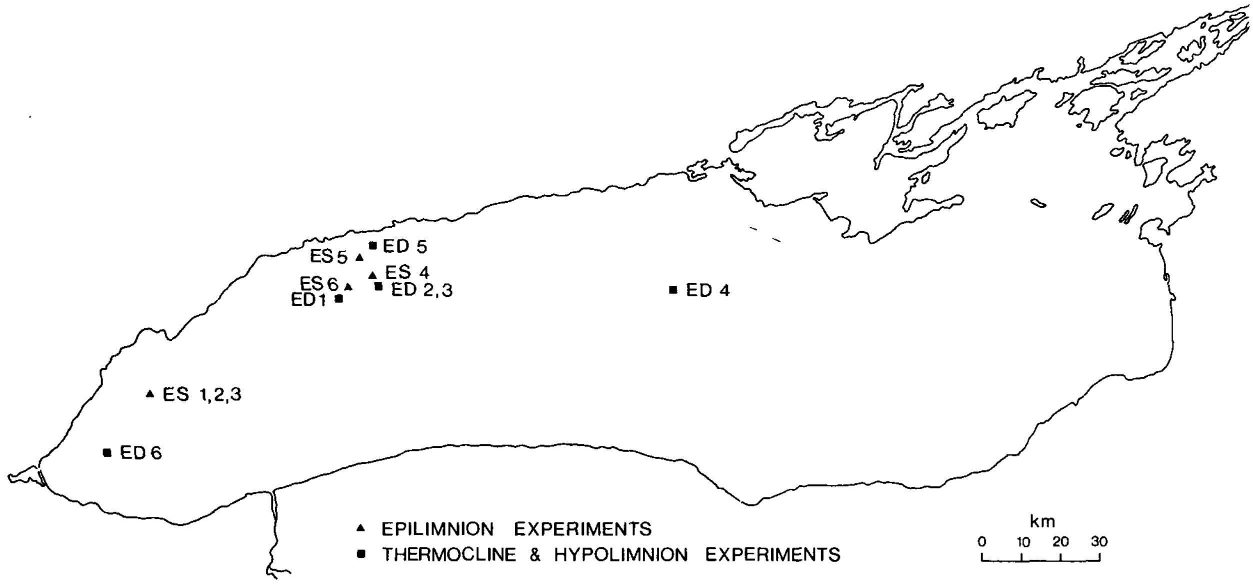

FIG. 1. Locations of dye diffusion experiments.

that all variations in both concentration and velocity may be neglected. However, the importance of vertical diffusion cannot be neglected even though the diffusing contaminant is, for practical purposes, confined to a very thin layer. The combined action of vertical shear in the horizontal mean current and vertical diffusion may produce considerable effective horizontal diffusion.

Horizontal distributions of dye concentration were prepared for each experiment from a good coverage of the dye patch during a reasonable sampling time interval and thus they could be treated as quasi-synoptic. The diffusion time is taken from the time of dye release to the middle of the time interval chosen for observing the horizontal distributions. The horizontal dye distributions are generally relative to a drogue (released with the dye) in a system moving with the mean current. It is usually not necessary to correct for translation during the sampling interval since the analysis of the data is carried out in a moving frame of reference (relative diffusion).

Typical horizontal concentration distributions constructed as lines of equal concentration are shown in Fig. 2.

The starting point in the analysis of field diffusion data is the calculation of the variances from the measured spatial concentration distributions of the dye patch. Often the measured concentration distributions are converted to equivalent radial symmetric distributions from which variances are calculated. It is implicit in such an analysis that the diffusion of the dye patch is governed by two-dimensional homogeneous turbulence.

The measured spatial concentration distributions are converted into equivalent radially symmetric distributions by defining the radius $r=(A_c/\pi)^{\frac{1}{2}}$ of a circle as a measure of the area A_c enclosed by a particular concentration contour C. Then the concentration distribution $C(r,t)$ characterized by the equivalent radii r and diffusion time t (i.e., time elapsed since dye release) would represent approximately the equivalent radially symmetric distribution. The variance $S_r^2(t)$ corresponding to the radially symmetric distribution $C(r,t)$ is given by

$$S_r^2(t)=\frac{\int_0^\infty r^2C(r,t)2\pi r dr}{\int_0^\infty C(r,t)2\pi r dr}. \tag{1}$$

TABLE 1. General details of epilimnion experiments.*

Experiment No.	Date	Duration (h)	Depth (m) of Dye	Thermocline	Bottom
ES 1	7 May 69	3.5	3	homogeneous	80
ES 2	17–18 Jun 69	30	3	10	80
ES 3	26–28 Aug 69	60	3	15	80
ES 4	30 May 72	4	3	3	46
ES 5	5 Jun 72	6	3	1–2	22
ES 6	27–29 Jun 72	53	3	3	73

* For locations see Fig. 1.

TABLE 2. General details of hypolimnion experiments.*

Experiment No.	Date	Duration (h)	Depth (m) of Dye	Thermocline	Bottom
ED 1	15–19 Aug 72	79	18–26	11	90–100
ED 2	29–30 Aug 72	30	35–45	7	85
ED 3	31 Aug–9 Sep 72	40	33–43	11	85
ED 4	6–8 Sep 72	60	25–35	14	110–120
ED 5	17–20 Oct 72	72	25–50	14	60–85

* For locations see Fig. 1.

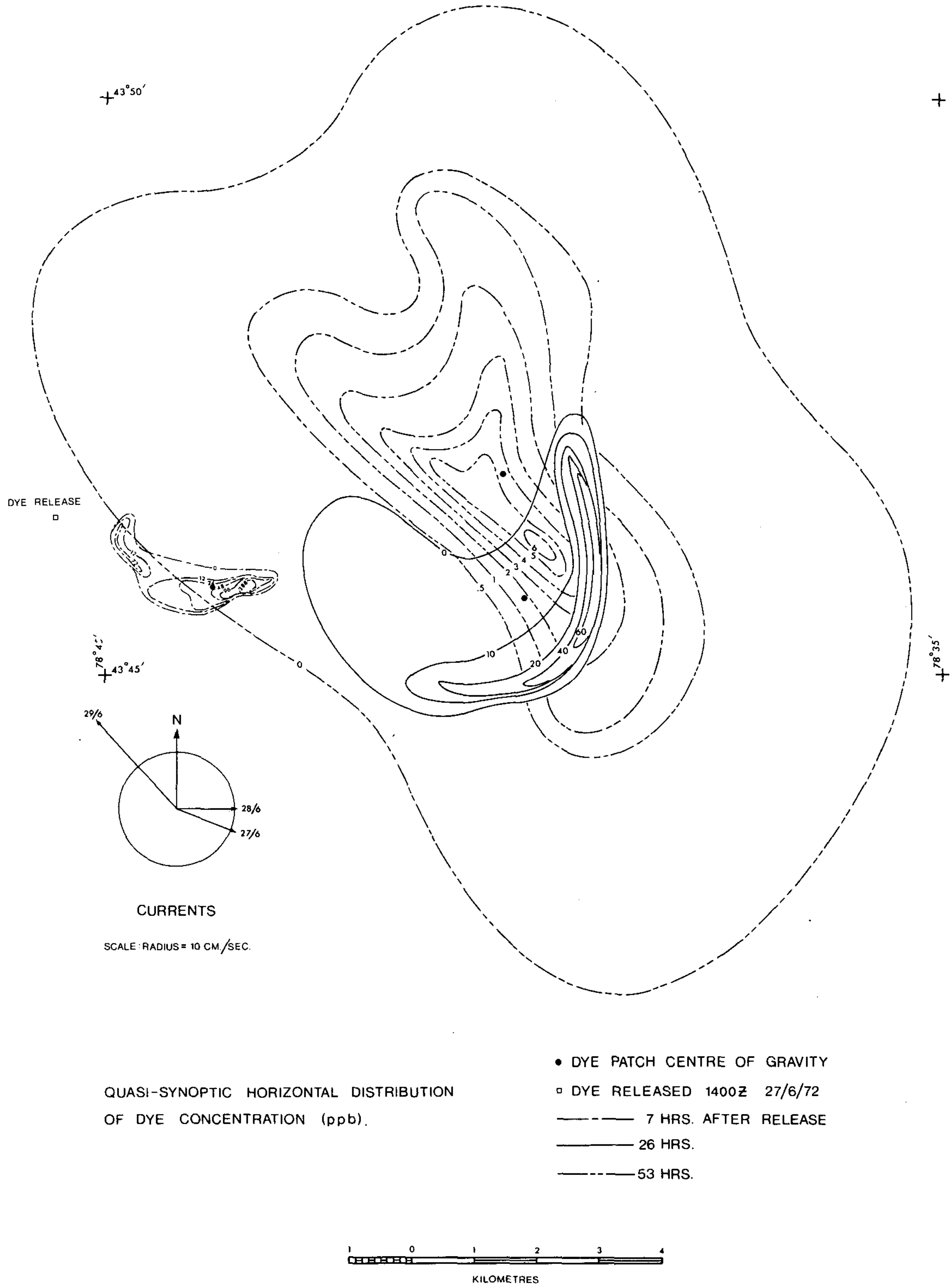

FIG. 2. Quasi-synoptic horizontal distribution of dye concentrations (ppb) at 3 m depth and at different times after dye release. Experiment ES6, 27–29 June 1972.

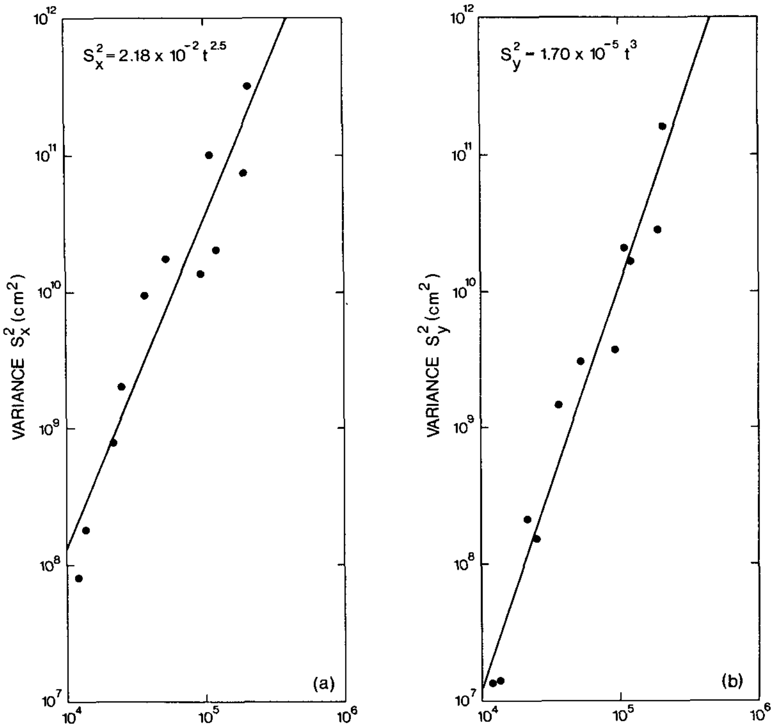

FIG. 3. Horizontal variance vs diffusion time: (a) longitudinal, (b) lateral.

The elongated appearance of the dye patch and the asymmetry in the observed concentration distributions do not support the radially symmetric hypothesis. Anisotropic turbulence (i.e., turbulent eddies which are more intense in the direction of the mean flow than across it) combined with "shear diffusion" due to vertical shear in the horizontal mean current, gives rise to enhanced mixing in the longitudinal direction. With these observed features in mind, the variances were computed by direct integration of the observed concentration distributions. Choosing a convenient rectangular coordinate system through the center of the distribution with the x axis in the direction of the mean current, the appropriate variances corresponding to a two-dimensional concentration distribution $C(x,y,t)$ are defined as follows:

Longitudinal

$$S_x^2(t)=\frac{1}{Q}\int\int_{-\infty}^{\infty} x^2C(x,y,t)dxdy \qquad (2)$$

Transverse

$$S_y^2(t)=\frac{1}{Q}\int\int_{-\infty}^{\infty} y^2C(x,y,t)dxdy \qquad (3)$$

For a two-dimensional elongated patch,

$$S_{xy}^2(t)=S_x^2(t)+s_y^2(t), \qquad (4)$$

where

$$Q=\int\int_{-\infty}^{\infty} C(x,y,t)dxdy. \qquad (5)$$

4. Diffusion characteristics

It is customary to interpret diffusion data and results from field experiments by constructing certain basic diffusion characteristics (Stommel, 1949; Okubo, 1971). A set of commonly used diffusion characteristics are the variance of the horizontal concentration distribution of the diffusing substance versus the diffusion time, and the eddy diffusivity versus the length scale of diffusion. A log-log plot of the variance against time determines a straight line which provides the empirical law

$$S^2=at^m. \qquad (6)$$

Assuming that the concentration distribution within the patch is isotropic, we can define an apparent diffusivity

$$K=\frac{1}{2}\frac{dS^2}{dt}. \qquad (7)$$

From (6) we have

$$K=(ma/2)t^{m-1}. \qquad (8)$$

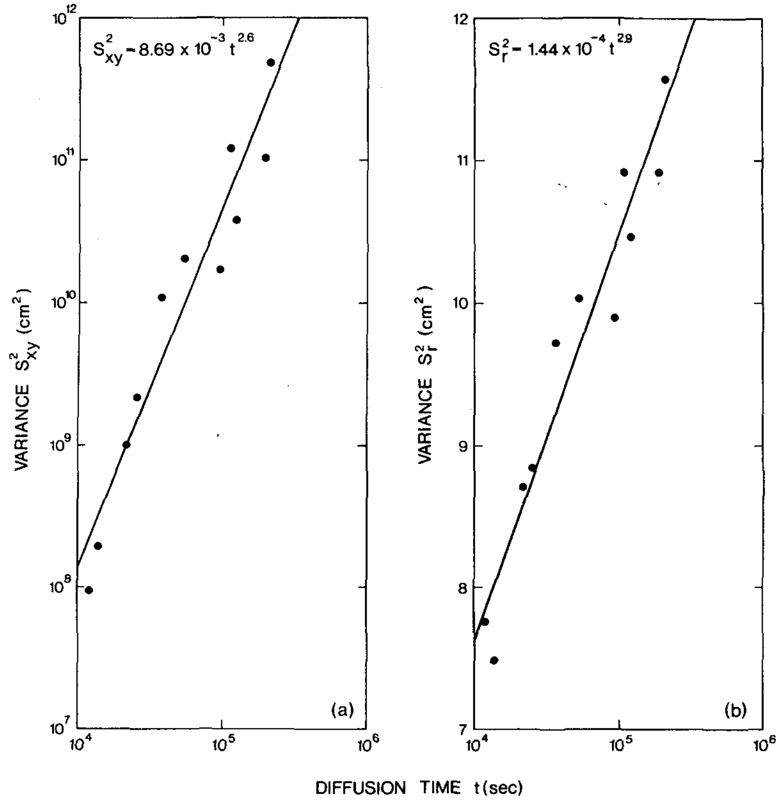

FIG. 4. As in Fig. 3 except for (a) a two-dimensional elongated patch, and (b) a radially symmetric patch.

Eliminating t from (6) and (8) yields

$$K = cS^n, \tag{9}$$

where $c = (m/2)a^{1/m}$ and $n = 2(m-1)/m$. Combining (6) and (9), some familiar diffusion characteristics can be deduced. From physical reasoning and dimensional considerations, m should be an integer. If $m=1$, then the variance grows linearly with the diffusion time scale which corresponds to the Fickian diffusion model with a constant diffusivity. If $m=2$, then the variance grows as the square of the time scale which corresponds to the shear diffusion model with a linear dependence of eddy diffusivity on length scale. If $m=3$, then the variance grows as the cube of the time scale corresponding to the inertial subrange diffusion with the familiar Richardson's "4/3 power law" dependence of eddy diffusivity on the length scale. A summary of these diffusion characteristics is given in Table 3.

Let us now examine the experimental data in the light of this simple theoretical framework. Figs. 3 and 4

TABLE 3. Summary of diffusion characteristics.

m	c	n	Diffusion law	Diffusion parameters	Diffusion model
1	$a/2$	0	$K \approx$ constant	constant diffusivity	Fickian diffusion
2	$a^{1/2}$	1	$K \sim q_s L$	q_s diffusion velocity L length scale	Shear diffusion
3	$1.5a^{1/3}$	$\frac{4}{3}$	$K \sim \epsilon^{1/3} L^{4/3}$	ϵ energy dissipation parameter L length scale	Inertial subrange diffusion

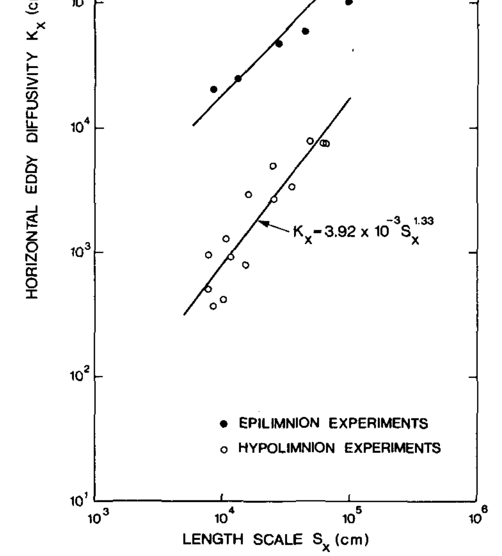

FIG. 5. Horizontal eddy diffusivity vs length scale of diffusion (longitudinal direction).

TABLE 4. Calculated variances and eddy diffusivities of epilimnion experiments.

Experiment No.	Diffusion time (s) t	Variances (cm²) S_x^2	S_y^2	S_{xy}^2	S_r^2	Eddy diffusivities (cm² s⁻¹) K_x	K_y	K_{xy}	K_r	K_x/K_y
ES1	1.2×10^4 (3.5 h)	8.01×10^7	1.36×10^7	9.38×10^7	5.7×10^7	1.99×10^4	2.49×10^3	2.33×10^4	7.96×10^3	7.99
ES2	1.1×10^5 (30 h)	1.01×10^{11}	2.07×10^{10}	1.21×10^{11}	8.32×10^{10}	4.84×10^5	1.91×10^5	7.22×10^5	4.91×10^5	2.53
ES3	3.69×10^4 (10 h)	9.40×10^9	1.468×10^9	1.09×10^{10}	5.28×10^9	1.00×10^5	2.25×10^4	1.33×10^5	6.43×10^4	4.44
	5.31×10^4 (15 h)	1.74×10^{10}	3.03×10^9	2.04×10^{10}	1.07×10^{10}	1.69×10^5	4.59×10^4	2.34×10^4	1.27×10^5	3.68
	1.22×10^5 (33 h)	2.04×10^{10}	1.66×10^{10}	3.82×10^{10}	2.94×10^{10}	5.61×10^5	2.34×10^5	8.48×10^5	5.95×10^5	2.40
	2.09×10^5 (60 h)	3.20×10^{11}	1.60×10^{11}	4.80×10^{11}	3.71×10^{11}	1.22×10^6	6.73×10^5	1.95×10^6	1.62×10^6	1.80
ES4	1.37×10^4 (4 h)	1.81×10^8	1.41×10^7	1.94×10^8	3.02×10^7	2.41×10^4	3.23×10^3	2.86×10^4	1.02×10^4	7.46
ES5	2.16×10^4 (6 h)	7.87×10^8	2.12×10^8	9.97×10^8	5.12×10^8	4.64×10^4	7.87×10^3	5.79×10^4	2.38×10^4	5.90
ES6	2.52×10^4 (7 h)	2.01×10^9	1.52×10^8	2.16×10^9	6.92×10^8	5.79×10^4	1.07×10^4	7.36×10^4	3.16×10^4	5.41
	9.36×10^4 (26 h)	1.35×10^{10}	3.65×10^9	1.71×10^{10}	7.87×10^9	3.83×10^5	1.39×10^5	5.62×10^5	3.63×10^5	2.76
	1.91×10^5 (53 h)	7.44×10^{10}	2.82×10^{10}	1.03×10^{11}	8.28×10^{10}	1.07×10^6	5.64×10^5	1.70×10^6	1.37×10^6	1.91

show log-log plots of variance as a function of the diffusion time scale. From a regression analysis of the computed variances and the diffusion time, the coefficient a and the exponent m were determined from (6). The regression analysis yields a value of m between 2 and 3 ruling out the Fickian diffusion model for time scales (and therefore the length scale) covered by these experiments. The eddy diffusivities were calculated using the corresponding values of a and m from (8). The computed variances and the corresponding diffusivities are summarized in Tables 4 and 5.

To construct the second set of diffusion characteristics, it is necessary to define the length scale of diffusion. The standard deviation S of the horizontal concentration distribution is a good measure of the length scale of diffusion (meaning that turbulent eddies of the size comparable to S are most effective in the diffusion of the dye patch). Figs. 5–8 show logarithmic plots of eddy diffusivity as a function of the corresponding length scale. The following regression equations were obtained defining the coefficient c and the exponent n in (9) [units—K: cm² s⁻¹; S: cm]:

Longitudinal

Epilimnion: $K_x = 8.75\times10^{-1} S_x^{1.07}$

Hypolimnion: $K_x = 3.92\times10^{-3} S_x^{1.33}$

Lateral

Epilimnion: $K_y = 7.05\times10^{-2} S_y^{1.26}$

Hypolimnion: $K_y = 1.59\times10^{-3} S_y^{1.38}$

Two-dimensional elongated patch (10)

Epilimnion: $K_{xy} = 5.58\times10^{-1} S_{xy}^{1.13}$

Hypolimnion: $K_{xy} = 2.15\times10^{-3} S_{xy}^{1.33}$

Two-dimensional equivalent radially symmetric patch

Epilimnion: $K_r = 1.8\times10^{-1} S_r^{1.2}$

Hypolimnion: $K_r = 8.2\times10^{-4} S_r^{1.4}$

Since the exponent m in (6) lies between 2 and 3 and is not explicitly defined, the exponent n is not clearly defined in accordance with any theoretical model.

As pointed out earlier, a very wide spectrum of horizontal motions exists in the Lakes. Thus the horizontal eddy diffusivity usually increases with the scale of mixing considered. As expected, however, the hypolimnion values are one to two orders of magnitude smaller than those of the epilimnion values. A plausible explanation for the smaller values at deeper depths could be that the available turbulent energy for diffusion decreases with depth.

It is of interest to compare the present data with oceanic data summarized by Okubo (1971). For such a

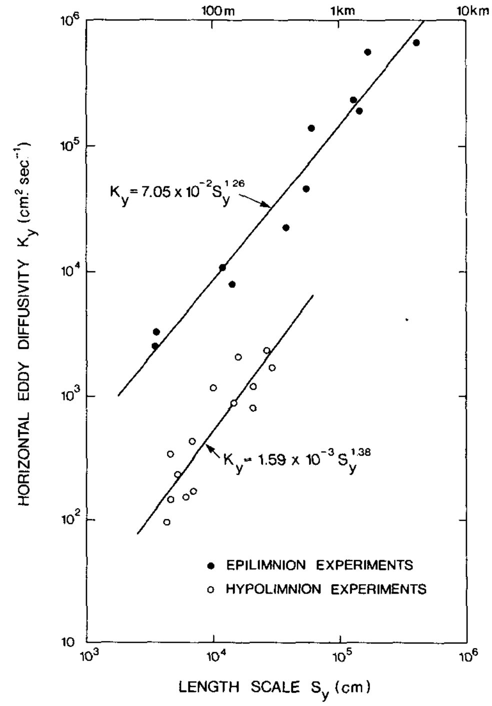

FIG. 6. As in Fig. 5 except for lateral direction.

TABLE 5. Calculated variances and eddy diffusivities of hypolimnion experiments.

Experiment No.	Diffusion time (s) t	Variances (cm²) S_x^2	S_y^2	S_{xy}^2	S_r^2	Eddy diffusivities (cm² s⁻¹) K_x	K_y	K_{xy}	K_r	K_x/K_y
ED1	4.3×10^4 (12 h)	1.1×10^8	4.6×10^7	1.56×10^8	8.3×10^7	1.28×10^3	4.35×10^2	9.07×10^2	4.83×10^2	2.94
	1.2×10^5 (33 h)	6.3×10^8	2.1×10^8	8.4×10^8	4.0×10^8	2.63×10^3	8.75×10^3	1.75×10^3	8.33×10^2	3.01
	1.8×10^5 (49 h)	1.2×10^9	4.3×10^8	1.63×10^9	4.9×10^8	3.33×10^3	1.19×10^3	2.26×10^3	6.81×10^2	2.80
	2.7×10^5 (74 h)	4.0×10^9	4.3×10^8	4.43×10^9	1.5×10^9	7.41×10^3	7.96×10^2	4.10×10^3	1.39×10^3	9.31
ED2	5.8×10^4 (16 h)	5.8×10^7	2.7×10^7	8.5×10^7	4.8×10^7	5.00×10^2	2.33×10^2	3.66×10^2	2.07×10^2	2.15
	7.2×10^4 (20 h)	1.3×10^8	2.1×10^7	1.51×10^8	8.3×10^7	9.03×10^2	1.46×10^2	5.24×10^2	2.88×10^2	6.18
ED3	3.1×10^4 (8.5 h)	5.9×10^7	2.1×10^7	8.0×10^7	4.6×10^7	9.52×10^2	3.39×10^2	6.45×10^2	3.71×10^2	2.81
	9.4×10^4 (26 h)	6.9×10^7	1.8×10^7	8.7×10^7	6.0×10^7	3.67×10^2	9.57×10^1	2.31×10^2	1.60×10^2	3.83
	1.4×10^5 (40 h)	2.2×10^8	4.8×10^7	2.68×10^8	1.6×10^8	7.86×10^2	1.71×10^2	4.79×10^2	2.86×10^2	4.60
ED4	1.2×10^5 (32 h)	1.0×10^8	3.7×10^7	1.37×10^8	4.6×10^7	4.17×10^2	1.54×10^2	2.85×10^2	9.58×10^1	2.71
ED5	4.3×10^4 (12 h)	2.5×10^8	1.0×10^8	3.5×10^8	2.5×10^8	2.91×10^3	1.16×10^3	2.03×10^3	1.45×10^3	2.51
	6.1×10^4 (17 h)	6.0×10^8	2.5×10^8	8.5×10^8	6.8×10^8	4.92×10^3	2.05×10^3	3.48×10^3	2.79×10^3	2.40
	1.5×10^5 (41 h)	2.3×10^9	7.0×10^8	3.0×10^9	2.3×10^9	7.67×10^3	2.33×10^3	5.00×10^3	3.83×10^3	3.29
	2.5×10^5 (68 h)	3.7×10^9	8.5×10^8	4.55×10^9	3.4×10^9	7.4×10^3	1.70×10^3	4.55×10^3	3.40×10^3	4.35

comparison, we use the diffusion parameters derived from radially symmetric distributions with the eddy diffusivity $K_r = S_r^2/4t$ and the length scale $L_r = 3S_r$ to be compatible with Okubo's summary. Fig. 9 shows log-log plots of both sets of data and considering that the experiments were conducted in a wide variety of environmental conditions, the Lake Ontario data compare favorably with the oceanic data. This would imply that the diffusion rate in the Lake is approximately the same as that of oceans.

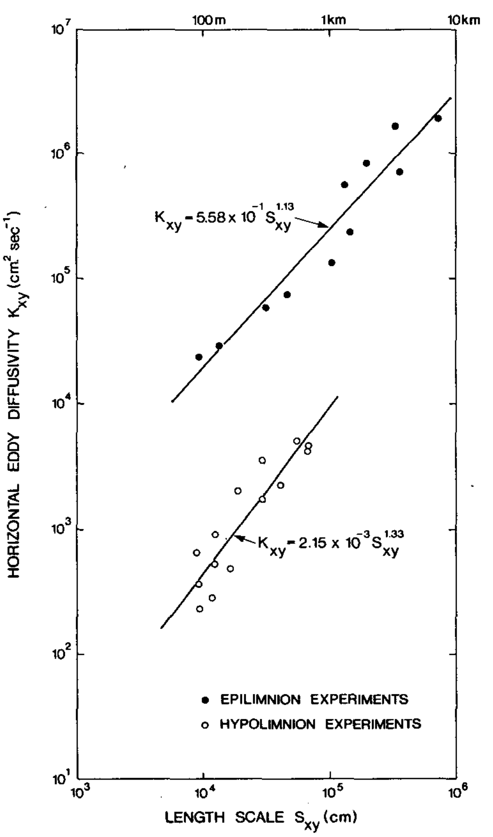

FIG. 7. As in Fig. 5 except for a two-dimensional elongated patch.

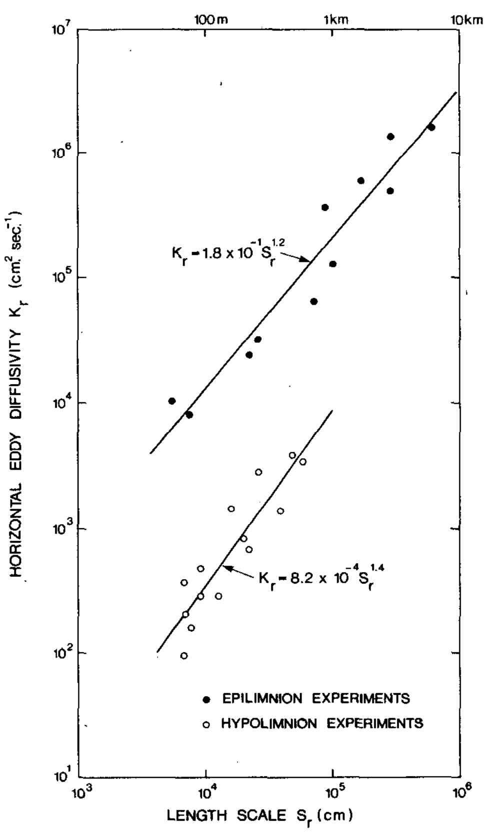

FIG. 8. As in Fig. 5 except for a two-dimensional radial symmetric patch.

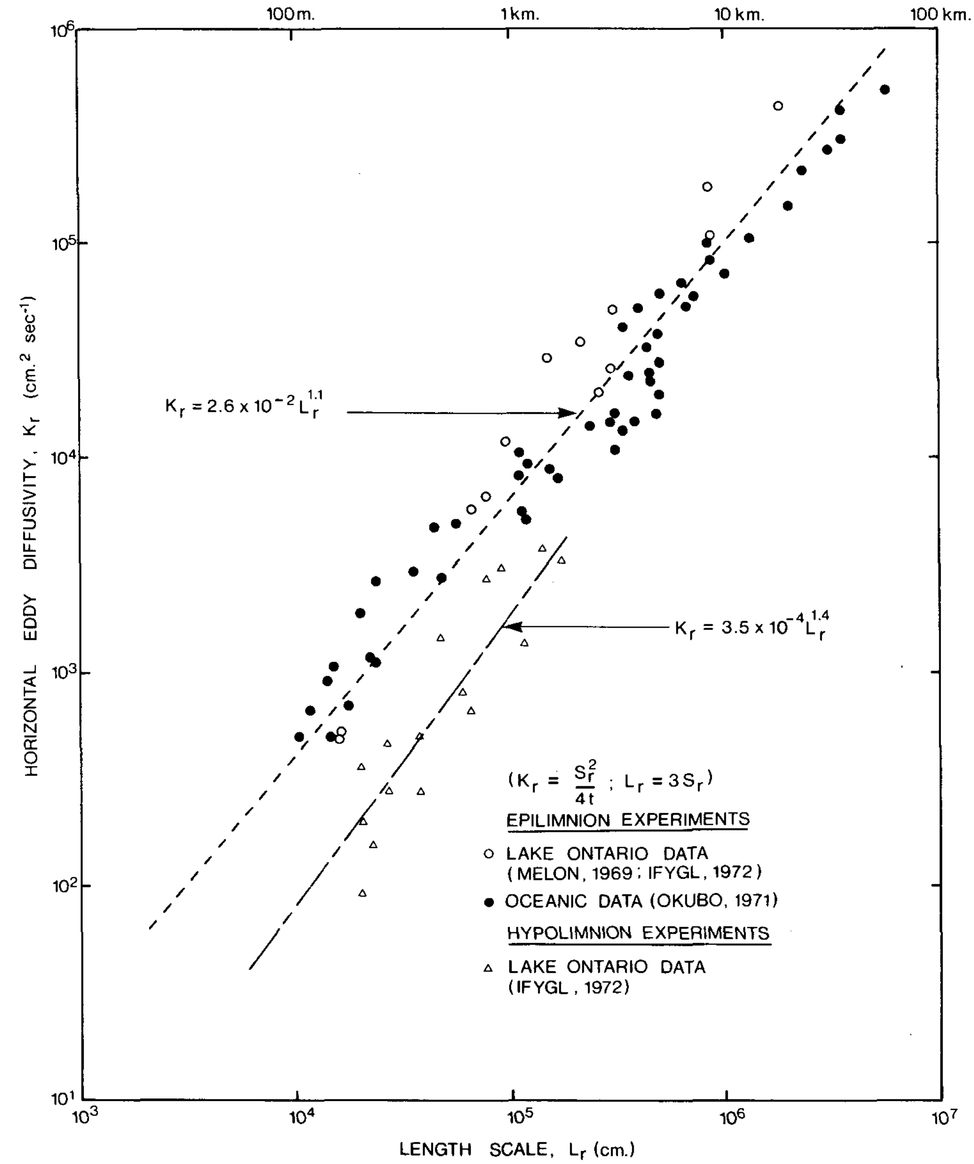

FIG. 9. Comparison of oceanic diffusion data (Okubo, 1971) with Lake Ontario diffusion data.

5. Conclusions

In general, the longitudinal eddy diffusivity K_x is greater by a factor of 5–10 in comparison with the lateral eddy diffusivity K_y during the initial stages of diffusion and by a factor of 2–3 for large diffusion times. During the initial stages of diffusion, when the dye patch is small (order of hundreds of meters), marked anisotrophy of turbulence, combined with "shear diffusion" due to vertical shear in the horizontal mean current, gives rise to an apparent increase in the longitudinal diffusion of the dye patch, whereas for large diffusion times, when the patch grows to the size of kilometers, localized non-uniformities in the flow do not appear to influence the overall diffusion of the patch. Observed horizontal concentration distributions shown in Fig. 2 seem to strengthen this argument.

A serious shortcoming of the present analysis of the results is that the eddy diffusivity and the length scale are both derived from dye diffusion experiments. To be realistic, the turbulence parameters such as length scales, intensity of turbulence, rate of energy dissipation, and other environmental parameters governing the diffusion process should be derived from the measured flow characteristics during the diffusion experiment, in order to interpret the dependence of the eddy diffusivity on the governing environmental parameters. Such an analysis should be the next step in a continuing effort to understand the diffusion processes.

The main conclusion that can be drawn from the experimental results is that the eddy diffusivity grows faster than given by the Fickian model and somewhat slower than in the "inertial subrange." Although the diffusion characteristics cannot be justified entirely from theoretical arguments, they could be viewed as purely statistical (or as a parameterization) since they have been constructed from experimental data obtained in widely varying environmental conditions. The dependence of the horizontal eddy diffusivity on the length scale provides a useful guideline for modeling practical diffusion problems.

Acknowledgments. The field work was organized and supervised by Mr. K. C. Miners, whose resourcefulness and persistence was responsible for the success of the experiments.

REFERENCES

Kullenberg, G., 1971: Vertical diffusion in shallow waters. *Tellus*, **23**, 129–135.

——, 1972: Apparent horizontal diffusion in stratified shear flow. *Tellus*, **24**, 17–28.

Murthy, C. R., 1970: An experimental study of horizontal diffusion in Lake Ontario. *Proc. 13th Conf. Great Lakes Res.*, Intern. Assoc. Great Lakes Res., 477–489.

——, 1973: Horizontal diffusion in lake currents. Publ. No. 109, Intern. Assoc. Hydrol. Sci., 327–334.

Okubo, A., 1971: Oceanic diffusion diagrams. *Deep-Sea Res.*, **18**, 789–802.

Stommel, H., 1949: Horizontal diffusion due to oceanic turbulence. *J. Marine Res.*, **8**, 199–225.